Cannabinoid action in the olfactory epithelium

Dirk Czesnik*†, Detlev Schild*‡, Josko Kuduz*, and Ivan Manzini*‡

*Department of Neurophysiology and Cellular Biophysics and ‡Deutsche Forschungsgemeinschaft Research Center for Molecular Physiology of the Brain, University of Göttingen, Humboldtallee 23, 37073 Göttingen, Germany

(Edited by L. L. Iversen, University of Oxford, Oxford, United Kingdom, and approved December 20, 2006 (received for review October 13, 2006)

The perception of odors is influenced by a variety of neuromodulators, and there is growing evidence that modulation already takes place in the olfactory epithelium. Here we report on cannabinergic actions in the olfactory epithelium of *Xenopus laevis* tadpoles. First we show that CB1 receptor-specific antagonists AM251, AM281, and LY320135 modulate odor-evoked calcium changes in olfactory receptor neurons. Second, we localize CB1-like immunoreactivity on dendrites of olfactory receptor neurons. Finally, we describe the cannabinergic influence on odor-induced spike-associated currents in individual olfactory receptor neurons. Here we demonstrate that the cannabinergic system has a profound impact on peripheral odor processing and discuss its possible function.

CB1 antagonist | dendrite | modulation | odor processing | olfactory receptor neuron

Sensory olfactory information is crucial in several behavioral aspects of humans and animals, e.g., nutrition and reproduction. It is everyday experience that olfactory stimuli that are attractive before food intake may become neutral or even aversive after. Functional MRI in humans showed that the activation of an orbitofrontal cortex area upon stimulation with banana odor was diminished after bananas were eaten to satiety (1). At a more peripheral stage, in mitral cells of the rat olfactory bulb, the responsiveness to food odors decreased when rats were fed, whereas it increased after fasting (2, 3). Some modulation may even occur in the olfactory epithelium (OE). In hungry axolotls s-neuropeptide Y enhances EOG responses to L-glutamic acid and modulates the amplitude of a tetrodotoxin-sensitive inward current (4). s-neuropeptide Y generally appears to play an important role in the control of appetite and feeding (5, 6).

Recently, the endocannabinergic system (ECS) has also been shown to be involved in food intake and energy homeostasis (7). Because in different animal phyla the levels of endocannabinoids are increased under fasting conditions (8–11), endocannabinoids may act as orexigenic mediators. These observations, together with the role of olfaction in food detection, led us to investigate whether olfactory receptor neurons (ORNs) are modulated by the cannabinergic system, which clearly turned out to be the case.

Results

CB1-Specific Antagonists Reduce Odor-Evoked Calcium Changes in ORNs. A mixture of 19 amino acids (100 μM, AAMIX) applied to an acute slice preparation of the OE of *Xenopus laevis* tadpoles (12) led to a specific cellular response pattern (Fig. 1 *A* and *B*) (13, 14). Amino acids are well known olfactory stimuli in aquatic animals involved in feeding behavior (15–17), and they are known to activate a subset of ORNs in the OE of larval *X. laevis* (13, 14). The response time courses of four amino acid-sensitive ORNs are plotted in Fig. 1*C*. Shape and duration of the intracellular calcium transients were highly reproducible when the odorants were applied repeatedly.

After the identification of amino acid-sensitive ORNs we added the cannabinergic antagonist AM251 to the bath solution. After drug wash-in the latency of the response to AAMIX was markedly increased (Fig. 1*D*; AM251, 5 μM, red curves). The amplitude as well as the delay and the duration of the responses were modulated in a stereotypic way. The amplitudes decreased, whereas the delay and the duration of the responses increased. After 12 min of washout the odor responses recovered (green curves). The degree of the described effects varied from ORN to ORN (Fig. 1*D*). The CB1 antagonists AM281 and LY320135 gave similar results (data not shown). The above-described modulation was observed in a total of 182 ORNs (18 slices from 18 different animals). The antagonists were used at concentrations of 1, 5, 10, and 20 μM. After a washout period of $\approx$15 min, 8 of 8 ORNs (1 μM), 73 of 79 ORNs (5 μM), and 19 of 56 ORNs (10 μM) recovered. With 20 μM antagonist concentration none of the 39 ORNs showed a recovery.

Application of AM251/AM281 alone did not alter the $[Ca^{2+}]_i$ level (15 slices, concentration range from 1 μM to 100 μM) (Fig. 1*E1*). In addition, the coapplication of amino acids and AM251 did not change the amino acid response (Fig. 1 *E2* and *E3*). This excludes a direct effect of the antagonists on the olfactory receptor proteins.

Furthermore, we excluded the possibility of non-CB1-mediated actions of the antagonists used. We were able to show that the recovery time after AM281 (10 μM) application could be markedly shortened by addition of the highly specific CB1 receptor agonist HU210. At an antagonist concentration of 10 μM a recovery from the antagonist effect was never seen before 5 min of washout with bath solution alone (34 ORNs in three slices) (Fig. 2*A*), whereas addition of HU210 (20 μM) led to an almost complete recovery of amino acid responses after 2 min of washout (Fig. 2*B*). Similar results were obtained in 36 cells of three slices. In addition, HU210 increased the statistical frequency of recovering responses from 19 of 56 (33%) ORNs (five slices) to 36 of 36 (100%) ORNs (three slices).

Distribution of CB1 Receptors in the OE. Using immunohistochemistry we found CB1 receptor-like immunoreactivity (CB1-LI IR) in the OE of *X. laevis* tadpoles (anti-rat CB1 N terminus antibody, kindly gifted by K. Mackie, University of Washington, Seattle, WA). ORNs were visualized by biocytin fills of the olfactory nerve (see *Materials and Methods*). Fig. 3*A* shows the typical localization and shape of ORNs. The somata of the biocytin-avidin-stained cells are clearly located in the ORN layer.

CB1-LI IR is localized to dendritic structures mainly in the apical part of the OE (Fig. 3*B*). The white rectangle in Fig. 3*A* indicates the region shown at higher magnification in Fig. 3 *D–F*. Dendrites and somata of individual ORNs can be clearly identified, and the CB1-LI IR is clearly associated with the dendritic compartments (Fig. 3 *E* and *F*). Somata and axons show no immunostaining (Fig. 3*A*). The specificity of CB1-LI IR was confirmed by the absence of immunostaining in sections treated

Author contributions: D.C., D.S., and I.M. designed research; D.C., J.K., and I.M. performed research; D.C. and I.M. analyzed data; and D.C., D.S., and I.M. wrote the paper.

The authors declare no conflict of interest.

This article is a PNAS direct submission.

Abbreviations: OE, olfactory epithelium; ECS, endocannabinergic system; ORN, olfactory receptor neuron; AAMIX, mixture of amino acids; CB1-LI IR, CB1-like immunoreactivity.

†To whom correspondence should be addressed. E-mail: dczesni@gwdg.de.

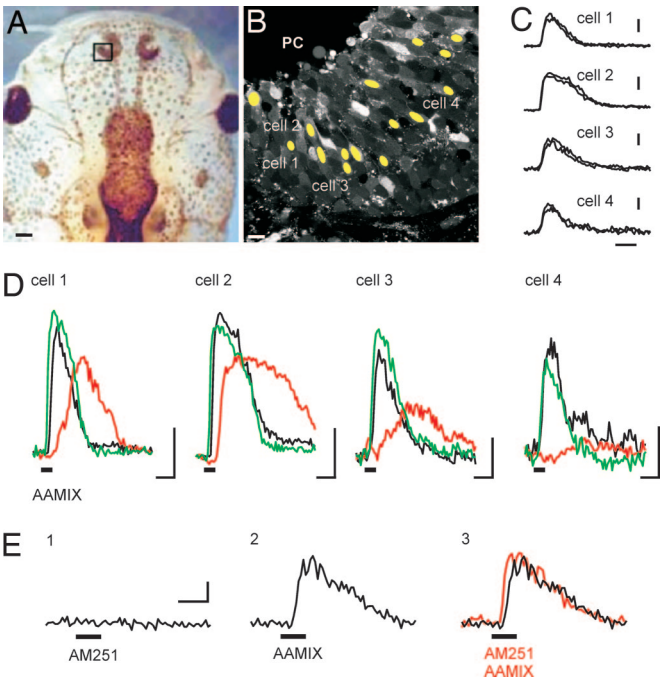

Fig. 1. AM251 alters odor-evoked $[Ca^{2+}]_i$ changes. (*A*) Overview of a *X. laevis* tadpole head. The black rectangle indicates part of the animal's left OE. (Scale bar: 500 μm.) (*B*) Fluo4-AM stained acute slice preparation of the OE (image acquired at rest). PC, principal cavity. The yellow ovals indicate the ORN somata of this slice that responded to the AAMIX (100 μM). (Scale bar: 10 μm.) (*C*) $[Ca^{2+}]_i$ transients of individual ORNs upon repeated applications of the AAMIX. The intraepithelial location of the four cells shown is indicated in *B*. [Scale bars: 10 s and $\Delta F/F$ 100% (cells 1 and 2) and 10 s and $\Delta F/F$ 50% (cell 3 and cell 4).] (*D*) After addition of AM251 (5 μM) to the bath solution the AAMIX-evoked ORN responses (black traces) were modulated (red traces). After 12 min of drug washout the odor-induced $[Ca^{2+}]_i$ transients recovered completely (green traces). [Scale bars: 10 s and $\Delta F/F$ 100% (cells 1 and 2) and 10 s and $\Delta F/F$ 50% (cells 3 and 4).] (*E*) AM251 does not interfere with odorant binding at olfactory receptors. Application of AM251 (50 μM) alone (*E1*) did not elicit any response. (*E2* and *E3*) Odorant-induced $[Ca^{2+}]_i$ transient upon application of the AAMIX (50 μM) alone (*E2*) and $[Ca^{2+}]_i$ transient induced by a coapplication of the antagonist (AM251, 50 μM) and 50 μM AAMIX (*E3*). The reproducibility of the $[Ca^{2+}]_i$ transients was not altered by the presence of the antagonist (compare black and red traces). (Scale bars: 10 s and $\Delta F/F$ 100%.)

with the anti-CB1 antibody preadsorbed with the immunizing fusion protein (Fig. 3*C*, as compared with Fig. 3*B*).

AM251 Alters Odor-Evoked On-Cell Spikes. The observed odorant-induced $[Ca^{2+}]_i$ changes in ORNs allow only indirect conclusions regarding the information conveyed to the olfactory bulb. We therefore tested the effect of the CB1-specific antagonists on odor-induced spiking activity by recording spike-associated currents of individual ORNs. Fig. 4*A1* shows a typical odor response of an individual ORN measured in the on-cell patch-clamp configuration. The poststimulus time histogram of the associated currents allows a comparison of repeated odorant responses (Fig. 4*B1*; first application, black curve; second application, red curve).

The application of AM251 (5 μM) increased the delay in the onset of the odor-induced spike-associated currents and the interspike interval of the responses (Fig. 4 *A2–A4* and *B2–B4*) although the stimulus was present at the OE for several seconds (Fig. 4*A6*). Similar results were obtained in seven other ORNs ($n = 7$ slices). Washout of the antagonists took some time so that a recovery could be observed only after ≈15 min (Fig. 4 *A5* and *B5*). Fig. 4*C* shows individual spike-associated currents at higher time resolution, each taken from the trace indicated. Amplitude and duration of the individual currents were not affected by the antagonists.

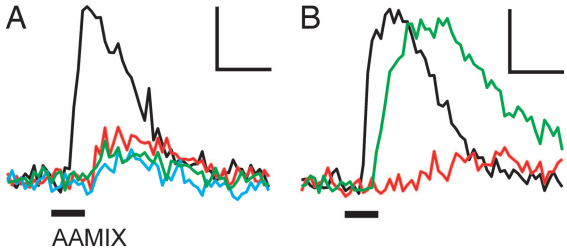

Fig. 2. CB1 receptor-mediated antagonist action upon amino acid-sensitive ORNs. (*A*) The modulatory effects of AM281 (10 μM; red trace) on an AAMIX-evoked ORN response (black trace) could not be washed out within 2 or 5 min with bath solution alone (green trace and blue trace, respectively). (*B*) $[Ca^{2+}]_i$ transient of an individual ORN upon application of the AAMIX (black trace). After addition of AM281 (10 μM) to the bath solution the AAMIX-evoked ORN response was suppressed (red trace). After 2 min of drug washout with HU210 (20 μM) in the bath solution, the odor-induced $[Ca^{2+}]_i$ transient recovered almost completely (green trace). [Scale bars: 10 s and $\Delta F/F$ 50% (*A*) and 10 s and $\Delta F/F$ 100% (*B*).]

Taken together, odor responses under CB1 antagonists are increasingly delayed with drug wash-in. While they are gradually more and more inhibited, they become longer-lasting and less intense (in terms of spikes per second). The effects of the CB1 antagonists on spiking activity are thus consistent with the effects on $[Ca^{2+}]_i$ above.

Discussion

In the present study we show the influence of the ECS on odor processing in the OE of *X. laevis* tadpoles. By means of confocal $[Ca^{2+}]_i$ imaging, patch clamp recordings, and immunohistochemistry we were able to locate the CB1 receptors and to describe the effects of CB1-specific antagonists.

In an acute slice preparation of the OE of *X. laevis* tadpoles we found that in ORNs the specific CB1 receptor antagonists AM251, AM281, and LY320135 decrease the amplitude of odor-evoked $[Ca^{2+}]_i$ traces and increase the latency to activation. We can exclude the possibility of a competitive antagonism of these drugs at the olfactory receptor proteins because (*i*) the antagonists showed the same effect, (*ii*) applying the drugs alone did not induce a response, and (*iii*) coapplication of a mixture of both amino acids and a high antagonist concentration never altered the amino acid-induced response.

Furthermore, we excluded any non-CB1-mediated effect of the used antagonists. We found that the highly specific CB1 agonist HU210 drastically accelerates the recovery during washout and increases the percentage of recovering responses.

CB1-LI IR is distributed mainly in the apical layer of the OE of *X. laevis* tadpoles, where generally both the dendrites of ORNs and the cell bodies of sustentacular cells are located (Fig. 3 *A* and *B*). Higher magnification together with visualization of ORN morphology by double staining with biocytin-avidin Alexa Fluor 488 allowed us to attribute the CB1-LI IR to ORN dendrites. ORN dendrites, which are present in all ORNs, from snails to humans, are certainly the appropriate compartment for partially decoupling the transduction compartment from the transformation compartment, and endocannabinoids may play a modulatory role in this compartment. Our evidence that CB1 receptors are located on the dendritic compartment and that CB1 antagonist application decreased responsiveness to odors is consistent with such a speculation.

Several studies show that CB1 receptors or the related mRNA occur at different stages of the central olfactory system in various animal phyla (18, 19). Our study extends this observation to the OE, the first stage of the olfactory system. Recent evidence

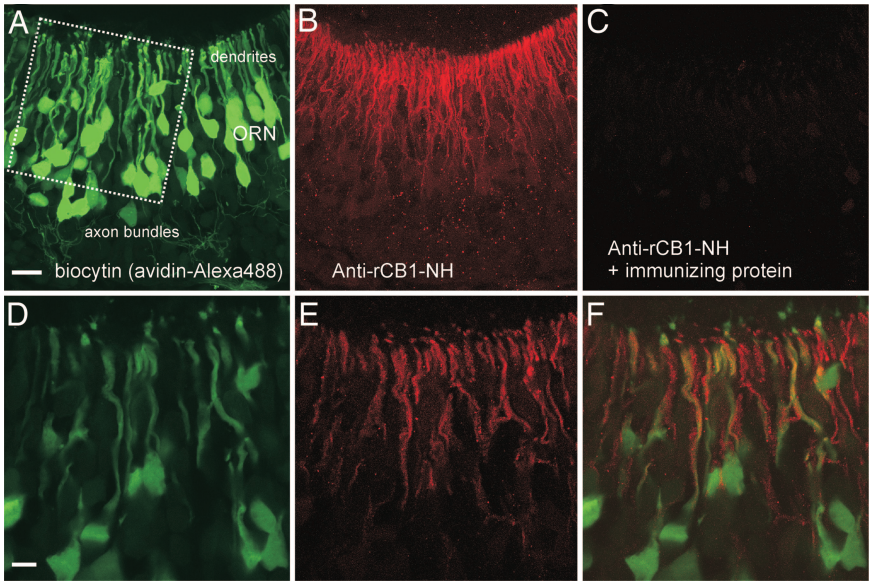

Fig. 3. CB1 distribution in the OE of *X. laevis* tadpoles. (*A*) Slice of an OE with biocytin-avidin-stained ORNs (merged z-stack; 16 optical slices, total thickness 14.4 μm). (Scale bar: 20 μm.) (*B*) Immunoreactivity to an rCB1-NH antibody of the same slice (see *Materials and Methods*). (*C*) Merged z-stack of an OE treated with the anti-CB1 antibody after preadsorption with the immunizing protein (see *Materials and Methods*). (*D–F*) Higher magnification of the region indicated by the white rectangle in *A* (merged z-stack; four optical slices, total thickness 3.6 μm). (Scale bar: 10 μm.) (*E*) CB1-LI IR localized to dendritic processes. The somata of the ORNs are clearly IR-free. (*F*) Overlay of *D* and *E*. CB1-LI IR is clearly occurring at ORN dendrites.

indicated the presence of CB1 mRNA in OE of *X. laevis* tadpoles at stage 46 (20). In our study we now describe the subcellular distribution of CB1 receptors in the OE of larval *X. laevis*. More importantly, we present the first physiological data of cannabinergic actions in ORNs upon odorant stimulation. Photon detection in the retina also seems to be modulated by the ECS (21–26). In addition, endocannabinergic signaling may also exist between taste cells and taste nerves (27). The endocannabinergic modulation of sensory output at the most peripheral stage may thus be a common feature of at least some sensory systems.

$[Ca^{2+}]_i$ imaging is a well established tool to reveal the sensitivity to odors (28), but it gives no direct information regarding whether the signal is relayed to higher brain centers. This can be concluded unambiguously only by directly measuring electrical activity of individual cells. We therefore recorded odor-induced trains of spike-associated currents. The observed modulatory effect by AM251 is comparable to the modulation detected in our $[Ca^{2+}]_i$ imaging experiments. Spiking responses were increasingly delayed, and they became longer and weaker, although the extent to which these effects occurred varied from ORN to ORN. Future experiments may show the relative contributions of the antagonist effects on response strength, its delay, and its length. In any case, it can already be stated with certainty that the cannabinergic system drastically alters the afferent input to the olfactory bulb.

AM251, AM281, and LY320135 act as both CB1-specific antagonists and inverse agonists (29). It has therefore to be clarified whether the observed modulation is due to a competitive antagonism or an inverse agonism. A tonic release of endocannabinergic substances may be assumed, because CB1 agonist application alone during repetitive odor application usually showed little or no effect (data not shown). Thus, the control of the endocannabinergic modulation of odorant-induced responses in ORNs needs to be investigated in more detail in future experiments. First steps in this direction would be a quantification of endocannabinoid levels in the OE combined with a detailed characterization of the involved mechanisms regarding re-uptake and enzymatic hydrolysis. Our finding that the ECS influences olfactory sensory input adds to a growing knowledge showing that the activity of ORNs is modulated by numerous compounds, including acetylcholine, adrenaline, ATP, dopamine, GnRH, and s-neuropeptide Y (4, 30–36).

Recently, several studies have been published dealing with the influence of the nutritious status on the neurophysiology of olfactory information processing and vice versa, whereby some of the phenomena could indirectly be attributed to the effects of modulators like orexin in the rat olfactory bulb or s-neuropeptide Y in the OE (4, 37–39). The ECS is also involved in food intake and energy homeostasis (7). For instance, in the teleost fish *Carassius auratus* (8), in the zebra finch (9), and in rodents (10, 11), brain endocannabinoids seem to act as orexigenic mediators. In addition, AM251 induces suppression of rat food intake and food-reinforced behavior (40). Thus, our findings together with the above-mentioned observations and the known role of olfaction in food detection support the view that the ECS may play an important role in the response of organisms to their nutritional status, which has to be clarified in future studies.

Materials and Methods

Slice Preparation for Calcium Imaging and Patch Clamping. Tadpoles of *X. laevis* (stages 51–54) (41) were chilled in a mixture of ice and water and decapitated, as approved by the University of Göttingen Committee for Ethics in Animal Experimentation. A block of tissue containing the OE, the olfactory nerves, and the brain was cut out and kept in bath solution (see below). The tissue was then glued onto the stage of a vibroslicer (VT 1000S; Leica, Bensheim, Germany) and cut horizontally into 130- to 150-μm-thick slices. For patch clamping the slices were placed under a grid in a recording chamber and viewed by using Nomarski optics (Axioskop 2; Zeiss, Göttingen, Germany). For imaging $[Ca^{2+}]_i$ the tissue slices were incubated with 200 μl of a bath solution (see below) containing 50 μM fluo-4 AM (Molecular Probes, Leiden, The Netherlands) and 50 μM MK571 (Alexis Biochemicals, Grünberg, Germany). Fluo-4 AM was dissolved in DMSO (Sigma, Deisenhofen, Germany) and Pluronic F-127 (Molecular Probes). The final concentrations of DMSO and Pluronic F-127 did not exceed 0.5% and 0.1%,

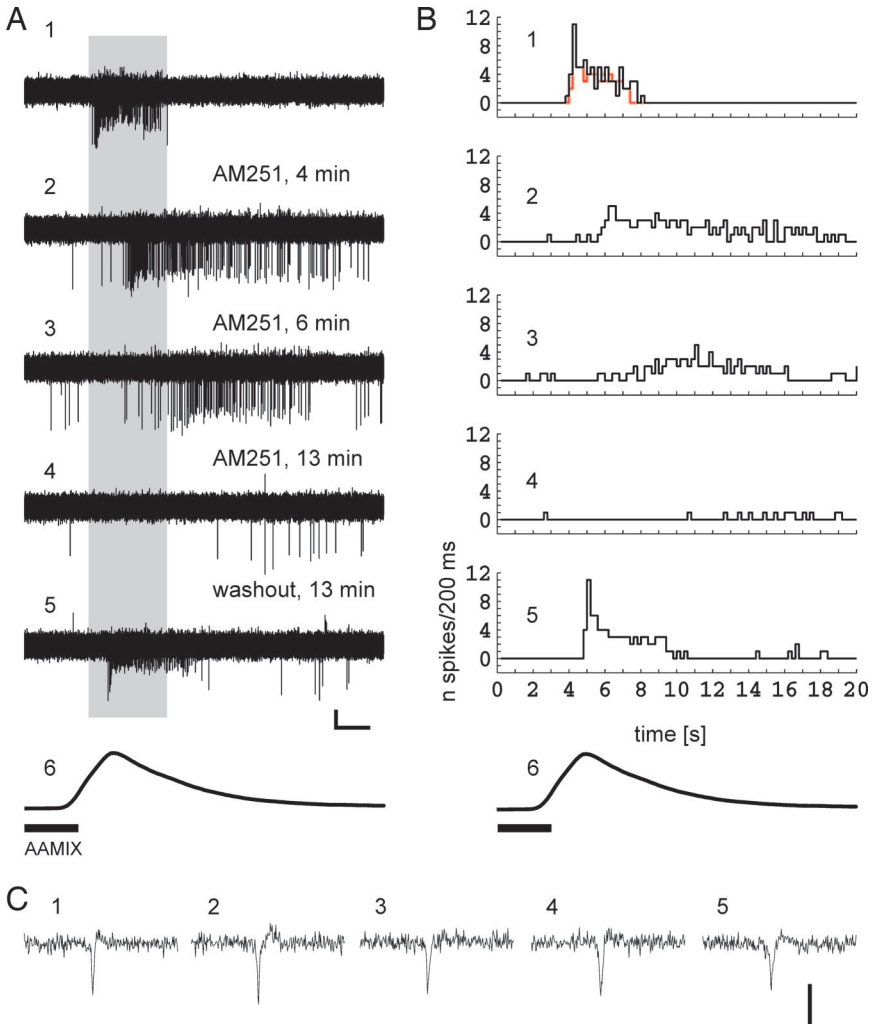

Fig. 4. CB1 antagonist AM251 alters odor-evoked electrical activity in individual ORNs. (*A1*) AAMIX-induced action potential-associated currents of an individual ORN. [Scale bars: 2 s and 20 pA (*A1–A5*).] The corresponding poststimulus time histogram is shown in *B1*. The superimposed red histogram comes from a successive AAMIX application (interstimulus interval 3 min; current trace not shown) and shows the high reproducibility of the odorant response. (*A2–A4* and *B2–B4*) The modulatory effect of AM251 on the action potential-associated currents depends on the wash-in time of the antagonist. (*A5* and *B5*) Recovery after 20-min drug washout. The time window of the original response is indicated by the gray-shaded area. (*A6* and *B6*) Odor concentration time course. Shown is simulation of the odor dynamics during a single odorant application (see *Materials and Methods*). (*C1–C5*) Zoom of individual spike-associated currents, one from each current trace *A1–A5* (trace duration 25 ms). (Scale bar: 40 pA.)

respectively. To avoid multidrug resistance transporter-mediated destaining of the slices, MK571, a specific inhibitor of the multidrug resistance-associated proteins, was added to the incubation solution (42). After incubation at room temperature for 35 min, the tissue slices were put under a grid in a recording chamber and placed on the microscope stage of an Axiovert 100M (Zeiss, Jena, Germany) to which a laser scanning unit (LSM 510; Zeiss) was attached. Before starting the calcium-imaging experiments, the slices were rinsed with bath solution for at least 15 min.

Calcium Imaging of Odor Responses. $[Ca^{2+}]_i$ was monitored by using a laser-scanning confocal microscope (LSM 510). The confocal pinhole was set to $\approx$140 μm to exclude fluorescence detection from more than one cell layer. Fluorescence images (excitation at 488 nm; emission $>$ 505 nm) of the OE were acquired at 1.27 Hz, with three to five images taken as control images before the onset of odor delivery. The fluorescence changes $\Delta F/F$ were calculated for individual ORNs as $\Delta F/F = (F_1 - F_2)/F_2$, where F_1 was the fluorescence averaged over the pixels of an ORN soma and F_2 was the average fluorescence of the same pixels before stimulus application, averaged over three images. A response was assumed if the following two criteria were met: (*i*) the first two intensity values after stimulus arrival at the mucosa, $\Delta F/F(t_1)$ and $\Delta F/F(t_2)$, had to be larger than the maximum of the prestimulus intensities; and (*ii*) $\Delta F/F(t_2) > \Delta F/F(t_1)$ with $t_2 > t_1$. Data analysis was performed with Matlab (Mathworks).

Patch Clamp Recordings. Patch electrodes with a tip diameter of 1–2 μm and $\approx$7–10 MΩ resistance were fabricated from borosilicate glass with a 1.8-mm outer diameter (Hilgenberg, Malsfeld, Germany) by using a two-stage electrode puller (Narishige, Tokyo, Japan). "On-cell configuration" recording of a cell was done after a gigaohm seal was obtained between the patch pipette and the membrane of an individual intact cell. This noninvasive technique makes it possible to record action potential-equivalent charge displacements of the membrane of an individual cell without affecting the composition of its intracellular solution (43). Holding voltage was 0 mV. Pulse protocols, data acquisition, and evaluation programs were written in C.

Voltage pulses were delivered from a microcontroller to a D/A converter and then to the patch clamp amplifier (EPC7; List, Darmstadt, Germany). The data were digitized online. Further data analysis was performed with Matlab.

Solution and Stimulus Application. The composition of the bath solution was 98 mM NaCl/2 mM KCl/1 mM $CaCl_2$/2 mM $MgCl_2$/5 mM glucose/5 mM sodium pyruvate/10 mM Hepes. The bath solution was also used as pipette solution for the on-cell recordings. The pH was adjusted to 7.8. The osmolarity of the solution was 230 mOsmol/liter. As odorants, we used the same mixture of 19 amino acids as in our previous work (12). The amino acids were dissolved in bath solution (stocks of 10 mM) and used at a final concentration of 50–100 μM in all of the experiments. Stimulus solutions were prepared immediately before use by dissolving the respective stock solution in bath solution. The bath solution was applied by gravity feed from a storage syringe through a funnel drug applicator to the recording chamber. Stimuli were pipetted directly into the funnel without stopping the flow. Outflow was through a syringe needle placed close to the OE. The time course of stimulus arrival at the OE was simulated by applying the fluorescent dye avidin Alexa Fluor 488 as a dummy stimulus and by measuring the fluorescence after avidin Alexa Fluor 488 application to the funnel. The delay of stimulus arrival caused by the syringe, i.e., from pipetting into the funnel to concentration increase in the OE, was $\approx$2 s (see Fig. 4*A*). The minimum interstimulus interval between odorant applications was at least 2 min. All of the chemicals were purchased from Sigma if not otherwise indicated. The CB1 receptor drugs AM251, AM281, LY320135, and HU210 (Tocris, Bristol, U.K.; stocks of 10 mM or 20 mM, 100% DMSO) were dissolved in bath solution and used at final concentrations indicated in *Results* or the figure legends.

Immunohistochemistry. ORNs of *X. laevis* tadpoles (stages 51–54) (41) were backfilled with biocytin (Molecular Probes) through the olfactory nerve. A crystal of biocytin was put into the nerve of anesthetized tadpoles. After the lesion was closed with histoacryl glue, the tadpoles were put back into the aquarium. Two hours later the tadpoles were chilled again and a block of tissue containing the OE was cut out, transferred into a solution of 4% formaldehyde in PBS (pH 7.4), and fixed for 2 h at room temperature. The tissue was then washed at least three times in PBS, embedded in 5% low-melting-point agarose (Agarose type II; Amreso, Solon, OH), and sectioned at $\approx$70 μm on a vibroslicer (VT 1000S). The slices were then immersed in a solution of avidin Alexa Fluor 488 conjugate (5 mg/ml; Molecular Probes) in PBS-TX (0.2%) overnight.

The OE slices were then double-stained with an affinity-purified primary polyclonal antibody raised against the N terminus of the rat CB1 receptor (rCB1-NH, raised in rabbit, kindly provided by Ken Mackie). We obtained the best results when sections were preincubated (1 h at room temperature) in TBS-TX and 2% normal goat serum (NGS) (ICN Biomedicals, Orsay, France). Background was reduced after preincubation in NGS. The tissue was then incubated overnight at 4°C with rCB1-NH (1:500) diluted in TBS-TX with 2% NGS. Sections were subsequently washed with TBS, and Alexa Fluor 546-conjugated anti-rabbit secondary antibody (Molecular Probes) was applied at a dilution of 1:250 in 1% NGS/TBS for 2 h at room temperature. The secondary antibody was washed off by five changes of TBS. The preparations were then transferred into 60% glycerol/PBS for at least 1 h and finally mounted on slides for confocal microscopy in 80% glycerol/PBS.

The specificity of the anti-CB1 antibody was previously assessed in rat (44) and evaluated in *X. laevis* tadpoles by incubating the sections with the anti-CB1 antibody (1:500) preadsorbed (1 h at room temperature) with the immunizing fusion protein (1 μg). Preparations were viewed by using a laser-scanning confocal microscope attached to an inverted microscope (LSM 510). Series of optical sections were imaged at intervals of 0.9 μm through the depth of the thick sections. They were saved as single optical images or three-dimensional stacks. Two-dimensional projections were generated for each channel and merged with the use of pseudocolors. Image processing was performed by using either Zeiss imaging software or GIMP (GNU Image Manipulation Program, www.gimp.org).

We thank Gudrun Federkeil for excellent technical assistance and Dr. Ken Mackie for generous supply of antibodies. This work was supported by grants from the Research Program of the Faculty of Medicine of Georg-August-Universität Göttingen (to D.C.) and the Deutsche Forschungsgemeinschaft Research Center for Molecular Physiology of the Brain (to D.S. and I.M.). Generation and purification of the rCB1-NH antibody was supported by the National Institutes of Health Grant DA11322.

1. O'Doherty J, Rolls ET, Francis S, Bowtell R, McGlone F, Kobal G, Renner B, Ahne G (2000) *NeuroReport* 11:399–403.
2. Chaput M, Holley A (1976) *Chem Senses* 2:198–201.
3. Pager J, Giachetti I, Holley A, Le Magnen J (1972) *Physiol Behav* 9:573–579.
4. Mousley A, Polese G, Marks NJ, Eisthen HL (2006) *J Neurosci* 26:7707–7717.
5. Kalra SP, Kalra PS (2004) in *Neuropeptide Y and Related Peptides,* ed Michel MC (Springer, Berlin), pp 221–249.
6. Levens NR, Feletou M, Galizzi JP, Fauchere JL, Della Zuana O, Lonchamt M (2004) in *Neuropeptide Y and Related Peptides,* ed Michel MC (Springer, Berlin), pp 283–235.
7. Matias I, Di Marzo V (2005) *Nat Neurosci* 8:585–589.
8. Valenti M, Cottone E, Martinez R, De Pedro N, Rubio M, Viveros MP, Franzoni MF, Delgado MJ, Di Marzo V (2005) *J Neurochem* 95:662–672.
9. Soderstrom K, Tian Q, Valenti M, Di Marzo V (2004) *J Neurosci* 24:10013–10021.
10. Kirkham TC, Williams C, Fezza F, Di Marzo V (2002) *Br J Pharmacol* 136:550–557.
11. Di Marzo V, Goparaju SK, Wang L, Liu J, Batkai S, Jarai Z, Fezza F, Miura GI, Palmiter RD, Sugiura T, Kunos G (2001) *Nature* 410:763–765.
12. Manzini I, Rössler W, Schild D (2002) *J Physiol* 545:475–484.
13. Manzini I, Schild D (2003) *J Physiol* 551:115–123.
14. Czesnik D, Kuduz J, Schild D, Manzini I (2006) *Eur J Neurosci* 23:119–128.
15. Sorensen, Caprio (1998) in *The Physiology of Fishes*, ed Evans DH (CRC, Boca Raton, FL), pp 251–261.
16. Valentincic T, Lamb CF, Caprio J (1999) *Physiol Behav* 67:567–572.
17. Nikonov AA, Finger TE, Caprio J (2005) *Proc Natl Acad Sci USA* 102:18688–18693.
18. Cesa R, Mackie K, Beltramo M, Franzoni MF (2001) *Cell Tissue Res* 306:391–398.
19. Egertova M, Elphick MR (2000) *J Comp Neurol* 422:159–171.
20. Beatrice M, Gabriella M, Francesca G, Oliana C (2006) *FEBS Lett* 580:1941–1945.
21. Straiker A, Stella N, Piomelli D, Mackie K, Karten HJ, Maguire G (1999) *Proc Natl Acad Sci USA* 96:14565–14570.
22. Straiker A, Sullivan JM (2003) *J Neurophysiol* 89:2647–2654.
23. Fan SF, Yazulla S (2003) *Vis Neurosci* 20:177–188.
24. Fan SF, Yazulla S (2004) *Vis Neurosci* 21:69–77.
25. Fan SF, Yazulla S (2005) *Vis Neurosci* 22:55–63.
26. Struik ML, Yazulla S, Kamermans M (2006) *Vis Neurosci* 23:285–293.
27. Oike H, Wakamori M, Mori Y, Nakanishi H, Taguchi R, Misaka T, Matsumoto I, Abe K (2006) *Biochim Biophys Acta* 1761:1078–1084.
28. Manzini I, Schild D (2004) *J Gen Physiol* 123:99–107.
29. Pertwee RG (2005) *Life Sci* 76:1307–1324.
30. Arechiga C, Alcocer H (1969) *Exp Med Surg* 27:384–394.
31. Bouvet JF, Delaleu JC, Holley A (1988) *Neurosci Res* 5:214–223.
32. Kawai F, Kurahashi T, Kaneko A (1999) *Nat Neurosci* 2:133–138.
33. Vargas G, Lucero MT (1999) *J Neurophysiol* 81:149–158.
34. Eisthen HL, Delay RJ, Wirsig-Wiechmann CR, Dionne VE (2000) *J Neurosci* 20:3947–3955.
35. Hegg CC, Greenwood D, Huang W, Han P, Lucero MT (2003) *J Neurosci* 23:8291–8301.
36. Hegg CC, Lucero MT (2004) *J Neurophysiol* 91:1492–1499.

37. Hardy AB, Aioun J, Baly C, Julliard KA, Caillol M, Salesse R, Duchamp- Viret P (2005) *Endocrinology* 146:4042–4053.
38. Apfelbaum A, Perrut A, Chaput M (2005) *Regul Pept* 129:49–61.
39. Caillol M, Aioun J, Baly C, Persuy MA, Salesse R (2003) *Brain Res* 960:48–61.
40. McLaughlin PJ, Winston K, Swezey L, Wisniecki A, Aberman J, Tardif DJ, Betz AJ, Ishiwari K, Makriyannis A, Salamone JD (2003) *Behav Pharmacol* 14:583–588.
41. Nieuwkoop PD, Faber J, eds (1994) *Normal Table of Xenopus laevis (Daudin)* (Garland, New York).
42. Manzini I, Schild D (2003) *J Physiol* 546:375–385.
43. Hamill OP, Marty A, Neher E, Sakmann B, Sigworth FJ (1981) *Pflugers Arch* 391:85–100.
44. Tsou K, Brown S, Saundo-Pena MC, Mackie K, Walker JM (1998) *Neuroscience* 83:393–411.